EVALUATION AND VERIFICATION OF THE TRIC SHELL ELEMENT

Pavlos Tsirigas, Andreas Gisakis, Vagelis Plevris, Manolis Papadrakakis

Institute of Structural Analysis & Seismic Research
School of Civil Engineering
National Technical University of Athens
Zografou Campus, 15780 Athens, Greece
e-mail: ptsirigas@gmail.com, {mpapadra, agisakis, vplevris}@central.ntua.gr;
web page: http://users.civil.ntua.gr/papadrakakis

Keywords: Shell element, Triangle, Verification, Membrane, Plane stress, Benchmark tests, Natural mode.

Abstract. *In the present work an investigation of the behavior of the improved shell finite element TRIC [1] is performed. The TRIC element is a simple yet sophisticated three-node shear-deformable isotropic and composite facet shell element that is suitable for large-scale linear or non-linear engineering computations of thin and moderately thick anisotropic plate and complex shell structures.*

The element formulation is based on the natural mode finite element method where the deformation or natural modes are separated from the rigid body modes. The element has substantial computational advantages, compared to the conventional isoparametric finite element formulation, such as analytical expressions for the computation of the stiffness matrix elements, shear locking-free properties and computational efficiency [2]. The improvement, which concerns the membrane (plane stress) behavior of the element, is achieved by applying an optimal method in calculating the elements of the stiffness matrix regarding the drilling degrees of freedom, while at the same time eliminating the aspect ratio locking of its predecessor.

The purpose of this work is to assess, via a thorough investigation, the ability of the improved element to address real-world structural problems in a computationally efficient and yet accurate way. For this purpose the behavior of the element is investigated in a number of benchmark tests. Both the stress and displacement fields of the element are tested. The results are compared with existing analytical solutions or with numerical results obtained from commercial finite element programs.

1 INTRODUCTION

An attempt to device a shell element with robustness, accuracy and efficiency has led to the derivation of the TRIC shell element [3,4]. A simple yet sophisticated triangular, shear-deformable facet shell element suitable for the analysis of thin and moderately thick isotropic as well as composite plate and shell structures. Its formulation is based on the natural mode finite element method [5], a method introduced by Argyris in the 1960s that separates the pure deformational modes - also called natural modes - from the rigid body movements of the element.

The TRIC element formulation can be decomposed in two different triangular elements. One for the pure-bending behavior and one for the membrane (plane stress) behavior. In a previous work [1], an enhancement of the element's membrane behavior was presented. The enhancement follows an optimal method in calculating the stiffness matrix regarding the rotational or drilling degrees of freedom (corner rotations normal to the plane of the shell element). The element performance in plane stress problems prior to the improvement was identical to that of the Constant Strain Triangle (CST) [6]. This element encounters great difficulties in determining the exact structural behavior, while it exhibits serious aspect ratio locking.

After a number of test examples, it was shown [1] that the new element exhibits substantial improvements compared to the original version. It is able to compute the correct solution with coarse meshes as well as with distorted elements (aspect ratio 16:1). It exhibits excellent performance in cases where all kinds of modes (membrane, bending and shear) are tuned simultaneously and cases where the mesh of the structure is quite distorted. Furthermore, the results obtained are very similar to those obtained with quadrilateral shell elements of commercial finite element programs.

The purpose of this work is to assess via a thorough investigation the ability of the improved element to address real-world structural problems in a computationally efficient and yet accurate way. Never before has the improved element been tested in conjunction with general purpose finite element prorgams. Also examples with temperature loading and z-axis eccentricity will de demonstrated. Furthermore, an attempt to derive two different elements, one pure membrane and one pure bending with only three degrees of freedom per node each, was made by deducting the three non-corresponding degrees of freedom from the shell element. Finally the

element behavior was tested in comparison to the beam theory by integrating the TRIC element stress field in various structural sections.

2 THE TRIC ELEMENT

The formulation of the TRIC shell element has been presented thoroughly in a number of papers [1-5]. In the present paper, due to length restrictions, only the basic features of the element will be highlighted and particularly those that are essential for the introduced examples.

2.1 Coordinate system of the element

The key-point for the formulation of the TRIC shell element is the adoption of the so-called natural coordinate system which has the three axes parallel to the sides of the triangle (α, β, γ). Apart from the natural system (α, β, γ) there are also the local elemental coordinate system (x΄, y΄, z΄) placed at the triangle's centroid, and the global Cartesian coordinate system (x, y, z). Finally, for each ply of the triangle, a material coordinate system (1, 2, 3) is defined with axis 1 being parallel to the direction of the material fibers.

2.2 Natural modes

In principle, the natural stiffness of an element is only based on deformation and not on associated rigid body motions. Thus, to the triangular shell element TRIC correspond 6 × 3 = 18 nodal displacements but only 18 - 6 = 12 independent straining modes can be derived in order to satisfy all kinematic compatibility conditions. The stiffness matrix $\mathbf{k}_N$ corresponding to these deformations is of dimensions 12 × 12 and is denoted as the natural stiffness matrix. A simple congruent transformation leads to the full 18 × 18 cartesian stiffness matrix of the element.

The 6 rigid-body and 12 straining natural modes of the TRIC element, can be grouped in the vector:

$$\underset{(18\times1)}{\boldsymbol{\rho}} = \left\{ \underset{(6\times1)}{\boldsymbol{\rho}_0} \quad \underset{(12\times1)}{\boldsymbol{\rho}_N} \right\}^T \left| \begin{array}{l} \boldsymbol{\rho}_0 = \left[\rho_{01} \quad \rho_{02} \quad \rho_{03} \quad \rho_{04} \quad \rho_{05} \quad \rho_{06} \right]^T \quad \textit{and} \\ \boldsymbol{\rho}_N = \left[\gamma_{ta}^0 \quad \gamma_{t\beta}^0 \quad \gamma_{t\gamma}^0 \quad \psi_{S\alpha} \quad \psi_{A\alpha} \quad \psi_{S\beta} \quad \psi_{A\beta} \quad \psi_{S\gamma} \quad \psi_{A\gamma} \quad \psi_{\alpha} \quad \psi_{\beta} \quad \psi_{\gamma} \right]^T \end{array} \right. \tag{1}$$

where $\boldsymbol{\rho}_0$ and $\boldsymbol{\rho}_N$ represent the rigid-body and straining modes, respectively.

2.3 Natural stiffness matrix ($\mathbf{k}_N$)

The components of the natural stiffness matrix are [1,2]:

$$\underset{(12\times12)}{\mathbf{k}_N} = \begin{bmatrix} \underset{(6\times6)}{\mathbf{k}_{qc}} & \mathbf{0} & \mathbf{0} \\ \mathbf{0} & \underset{(3\times3)}{\mathbf{k}_{qh}} & \mathbf{0} \\ \mathbf{0} & \mathbf{0} & \underset{(3\times3)}{\mathbf{k}_{az}} \end{bmatrix} \tag{2}$$

where: $\mathbf{k}_{qc}$ is the axial and symmetrical bending stiffness terms, $\mathbf{k}_{qh}$ is the anti-symmetrical bending and shear stiffness terms and $\mathbf{k}_{az}$ is the stiffness terms due to in-plane rotations (azimuth stiffness terms). The derivation of $\mathbf{k}_{qc}$ and $\mathbf{k}_{qh}$ has already been presented in [2] and the derivation of the improved $\mathbf{k}_{az}$ in [1].

3. COMPUTATIONAL TECHNIQUES

3.1 Temperature loading [3]

We formulate the Cartesian thermal load vector. For this purpose we shall adopt a linear through-the-thickness spatial temperature variation, namely:

$$T(x, y, z) = T_o(x, y) + zT_1(x, y) \tag{3}$$

where z is the distance from the elements center in the local cartesian system. The parameters T_o, T_1 in (3) are related to the temperatures at the top and bottom of a laminate T_t, T_b respectively, via:

$$T_0 = \frac{1}{2}(T_t + T_b) \quad , \quad T_1 = \frac{1}{h}(T_t - T_b) \tag{4}$$

where h represents the plate or shell thickness. The thermal load vector will be computed first in the natural

coordinate and then transformed first to the local and then to the global coordinates system before assembly. Thus, the natural thermal load vector J_N will be written as the sum of two vectors, namely:

$$\underset{(12\times1)}{J_N} = J_{N0} + J_{N1} \tag{5}$$

where J_{N0}, J_{N1} are the thermal loads due to uniform and linear through-the-thickness temperature distributions, respectively. To this end we define, for every layer, the thermoelastic coefficients in three coordinate systems, namely the material, the local elemental Cartesian and the natural coordinate system as:

$$\alpha_t^{123} = \begin{bmatrix} \alpha_{t_{11}} & \cdot \\ \cdot & \alpha_{t_{22}} \end{bmatrix}, \quad \left\{\alpha_t^{'}\right\}^T = \begin{bmatrix} \alpha_{xx} & \alpha_{yy} & \sqrt{2}\alpha_{xy} \end{bmatrix}, \quad \left\{\alpha_t\right\}^T = \begin{bmatrix} \alpha_{t\alpha} & \alpha_{t\beta} & \alpha_{t\gamma} \end{bmatrix} \tag{6}$$

In (6), α_{t11}, α_{t22} are the coefficients of thermal expansion along and perpendicular to the fiber direction, respectively, and are defined as input data. In the presence of temperature the total natural strain is the sum of the elastic and thermal strains:

$$\delta U = \int_V \sigma_c^t \delta\gamma_t dV = \int_V [\gamma_t^t - \eta_t^t]\kappa_{ct}\delta\gamma_t dV = \rho_N^t \left[\int_V \alpha_N^t \kappa_{ct}\alpha_N dV\right]\delta\rho_N - \underbrace{\left[\int_V \eta_t^t \kappa_{ct}\alpha_N dV\right]}_{\text{natural thermal load vector}}\delta\rho_N \tag{7}$$

Using the basic definition of thermal strain $n_t = a_t(T_0 + zT_1)$, the initial load due to temperature finally becomes:

$$J_N^t = J_{N0}^t + J_{N1}^t = \int_V [T_0\alpha_t^t\kappa_{ct}]\alpha_N dV + \int_V [zT_1\alpha_t^t\kappa_{ct}]\alpha_N dV \tag{8}$$

All integrals involved in the thermal energy statement (8) are calculated analytically, avoiding expensive numerical computations. Finally the computation of natural internal forces due to temperature loading is done via:

$$\underset{(18\times1)}{F_N^t} = \underset{(12\times12)}{\mathbf{k}_N^{-1}}\ \underset{(12\times1)}{J_N^t} \tag{9}$$

and they are obtained from the natural internal forces due to the structure's displacement field, to produce the final natural internal forces of the element.

3.2 Out of plane eccentricity

The reference surface of the TRIC shell element is defined by the shell's nodes and its surface direction. When modeling with shell elements, the reference surface is typically coincident with the shell's midsurface. However, many situations arise in which it is more convenient to define the reference surface as an offset from the shell's midsurface. The degrees of freedom for the shell are associated with the reference surface where all kinematic quantities are referred to. Any loading in the plane of the reference surface will, therefore, cause both membrane forces and bending moments when eccentricity is present.

The eccentricity can be positive or negative and is equal to the distance z_e from the shell's midsurface to the reference surface measured on the elements local z coordinate axis. The relation among the reference local coordinate system and the midsurface local coordinate system is defined by the transformation matrix T_e. In case of equal z eccentricity for all nodes the matrix T_e is equal to:

$$\underset{(18\times18)}{T_e} = \begin{bmatrix} T_e^{node1} & 0 & 0 \\ 0 & T_e^{node2} & 0 \\ 0 & 0 & T_e^{node3} \end{bmatrix}, \quad \text{where} \quad \underset{(6\times6)}{T_e^{nodei}} = \left[\begin{array}{c|ccc} & 0 & z_e & 0 \\ \underset{(3\times3)}{I} & -z_e & 0 & 0 \\ & 0 & 0 & 0 \\ \hline \underset{(3\times3)}{0} & \multicolumn{3}{c}{\underset{(3\times3)}{I}} \end{array}\right] \tag{10}$$

3.3 Membrane or plate only element formulation

TRIC, as a shell element, can be regarded as a combination of a membrane and a plate element that is subjected to extension and flexure, respectively. Its membrane behavior is represented by six translational nodal degrees of freedom in the plane of the triangle and three out of plane rotational degrees of freedom, one for each node, while its flexural behavior is described by nine degrees of freedom, one out-of-plane translation and two rotations for each node.

From equation (2) we deduce that the coupling terms between the components of the natural stiffness matrix are equal to zero which attests that the stiffness matrix can be divided in any of the individual coupling terms without performing static condensation. Furthermore, in case of material isotropy the axial and symmetrical

bending stiffness terms $\mathbf{k}_{qc}$ have also no coupling terms between them:

$$\underset{(6\times6)}{\mathbf{k}_{qc}} = \begin{bmatrix} \underset{(3\times3)}{\mathbf{k}_{ta}} & 0 \\ 0 & \underset{(3\times3)}{\mathbf{k}_{Sa}} \end{bmatrix} \tag{11}$$

Taking the above remarks into consideration it is clear that the elements natural stiffness matrix can be decomposed in two different stiffness matrices, one only for a membrane element $\mathbf{k}_N^m$ and one only for a bending element $\mathbf{k}_N^b$:

$$\underset{(6\times6)}{\mathbf{k}_N^m} = \begin{bmatrix} \underset{(3\times3)}{\mathbf{k}_{ta}} & 0 \\ 0 & \underset{(3\times3)}{\mathbf{k}_{az}} \end{bmatrix}, \quad \underset{(6\times6)}{\mathbf{k}_N^b} = \begin{bmatrix} \underset{(3\times3)}{\mathbf{k}_{Sa}} & 0 \\ 0 & \underset{(3\times3)}{\mathbf{k}_{qh}} \end{bmatrix} \tag{12}$$

Following the same methodology as with the full shell element [1,2,3], these two submatrices lead to the creation of two subelements with pure membrane or bending behavior.

4 NUMERICAL TESTS

For the comparisons we used HKS ABAQUS v6.4 [7] (S3R general purpose triangle shell element) and MSC NASTRAN 2004 [8] (CTRIA3 general purpose triangle shell element, CTRIAR improved membrane triangle shell element, CQUAD4 general purpose quadrilateral shell element, CQUADR improved membrane quadrilateral shell element and CBEAM 2-node linear beam). All the obtained results from the improved TRIC element came from the commercial structural analysis program FESPA (LH Logismiki), after the successful implementation of the TRIC element into it. The beam element used in conjunction with the improved TRIC is a 2-node linear isoparametric beam, included in FESPA.

4.1 Patch test (membrane mode)

4.1.1 Model properties

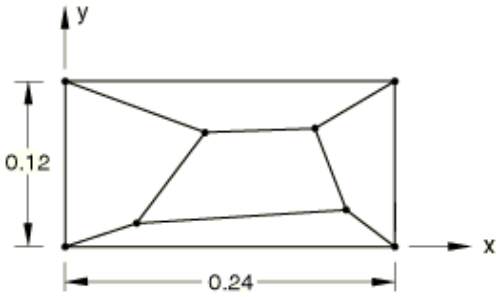

Figure 1. Model for numerical test 1

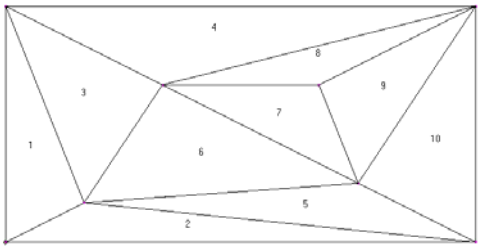

Figure 2. FE mesh for numerical example 1

The thickness of the membrane is t = 0.001, while the material Modulus of Elasticity is E = 1.0×10^6 and the Poisson ratio is ν = 0.25. Out of plane displacement $U_z = 0$ is enforced for all nodes, while an in-plane displacement field is applied as a boundary condition for all the edge nodes: $U_x = 10^{-3}((x+y/2)$, $U_y = 10^{-3}(y+x/2)$.

4.1.2 Results

Analytical solution by MacNeal, R.H., Harder, R.L. [9]: Stress $\sigma_{xx} = \sigma_{yy} = 1333$ and $\tau_{xy} = 400$ for all elements. Results for TRIC element: $\sigma_{xx} = \sigma_{yy} = 1333.33$, $\tau_{xy} = 400.00$ for all elements. The results of the two programs coincide.

4.2 Shear wall under bending or membrane loading

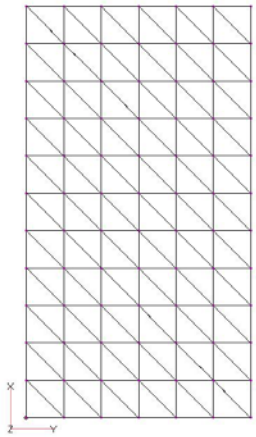

Figure 3. Model for numerical test 2

Geometry
Width of wall: L = 5.00 m
Height of wall: H = 9.20 m
Thickness of wall: t = 0.40 m

Material
Modulus of elasticity: E = 32 GPa
Poisson ratio: ν = 0.30

Constraints
Fixed constraints at the base of the wall.

Mesh
Structured mesh. Element width 0.83 m.

In this test example, the finite element results are compared to a beam model results. In order to calculate the equivalent axial force, shear force and bending moment along a given section of the model, the finite element results are integrated along the section.

4.2.1 Loading a – Pure bending mode

A total load F_z = -70 kN is applied with 7 nodal elements (10 kN each) on the top nodes (x = 9.2 m). A beam model (cantilever) with force F_z at the top yields the following: Shear force distribution: $V_z(x) = F_z$, Bending moment distribution: $M_y(x) = F_z \cdot x$.

Results and comparison

	Base		**Middle**		**Top**	
	Analytical solution	TRIC (integration)	Analytical solution	TRIC (integration)	Analytical solution	TRIC (integration)
$\mathbf{V_z}$ (kN)	-70.00	-68.08	-70.00	-70.68	-70.00	-71.19
$\mathbf{M_y}$ (kN·m)	612.50	612.17	321.30	321.21	29.40	29.86
$\mathbf{M_x}$ (kN·m)	0.00	-2.64	0.00	-0.90	0.00	-1.59

4.2.2 Loading b – Pure membrane mode

A total load F_y = -70 kN applied with 7 nodal elements (10 kN each) on the top nodes (x = 9.2 m). The beam model (cantilever) with force F_x at the top yields the following: Shear force distribution: $V_y(x) = F_y$, Bending moment distribution: $M_z(x) = F_y \cdot x$.

Results and comparison

	Base		**Middle**		**Top**	
	Analytical solution	TRIC (integration)	Analytical solution	TRIC (integration)	Analytical solution	TRIC (integration)
$\mathbf{V_z}$ (kN)	-70.00	-69.58	-70.00	-70.02	-70.00	-70.67
$\mathbf{M_y}$ (kN·m)	0.00	0.43	0.00	1.09	0.00	1.76
$\mathbf{M_x}$ (kN·m)	-612.50	-620.18	-321.30	-327.61	-29.40	-33.48

4.2.3 Deformed shapes and Von Mises stress for both loading cases

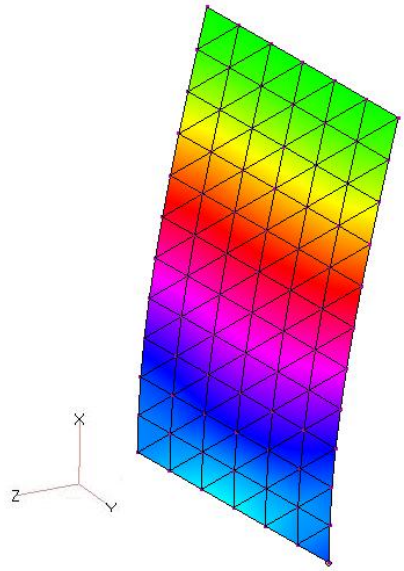

Figure 4. Deformed shape for loading a, Von Mises stress (upper surface)

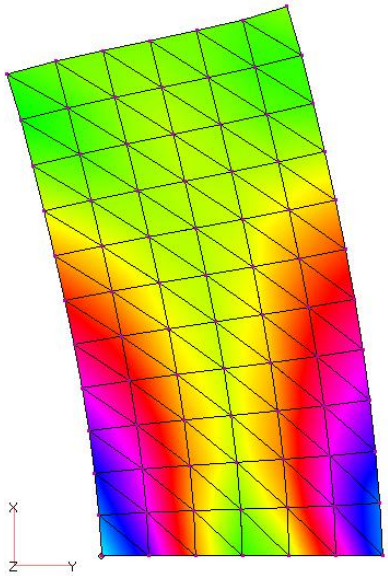

Figure 5. Deformed shape for loading b, Von Mises stress (upper surface)

4.3 Plate under bending loading

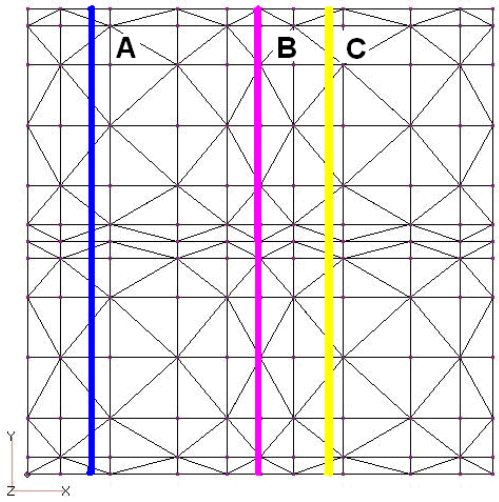

Figure 6. Model and sections for numerical test 3

Geometry
Dimensions: $L_x = L_y = 6.00$ m
Thickness: h = 0.20 m

Material
Modulus of elasticity: E = 32.0 GPa
Poisson ratio: ν = 0.0.

Constraints
Fixed constraint (6 DOFs) on the two edges with y = 0.0 m and y = 6.0 m.

Loading
Uniform loading: 10 kN/m^2 on all the surface (total load 360 kN) on direction –Z.

4.3.1 Analytical solution

The analytical solution can be obtained by a beam approach:

	Moment M_x (kN·m)	**Shear force V_z (kN)**
y=0.0 m and y=6.0 m	-30.00	+30.00 / -30.00
y=3.0 m	15.00	0.00

4.3.2 Sections and results

On a section parallel to X-axis no bending moment is expected regardless of Y. On the middle (Y=3.00 m) no shear force V_z, is expected (Poisson ratio ν = 0).

Three sections were examined (A, B, C), as shown in figure 6.

For each section the bending moment and shear force diagrams are presented per unit length of the section.

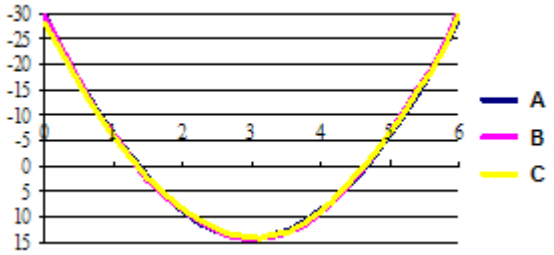

Figure 7. Bending moment diagramms M_x (kN·m) per unit length of the section.

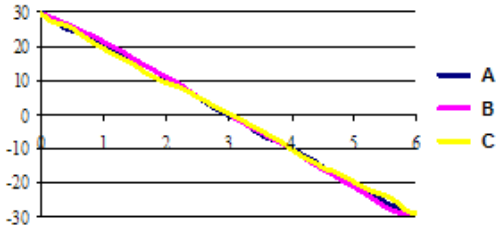

Figure 8. Shear force diagrams V_z (kN) per unit length of the section.

For sections A, B and C the horizontal axis is the distance from y = 0.00 m to y = 6.00 m. The diagrams give the same results as the analytical solution.

4.4 Connection of shells with beam linear elements – Combined bending and membrane loading

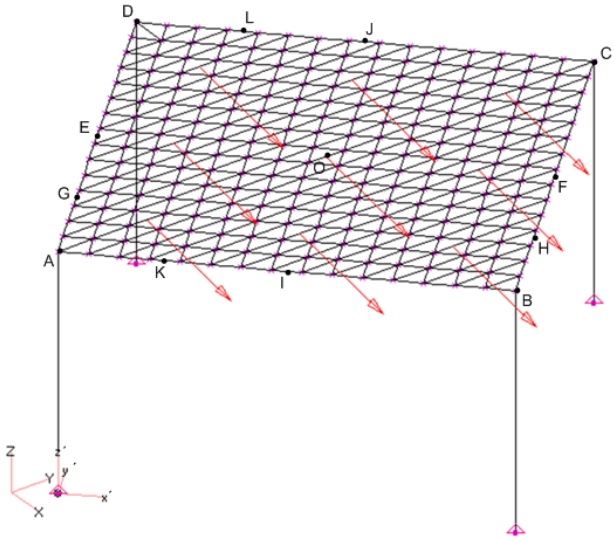

Figure 9. Model for numerical test 4

Plate properties
Length , width: L = 5.00 m
thickness: t = 0.30 m
Modulus of elasticity:
E = 30 GPa, Poisson ratio: ν = 0.3

Beams: Section 0.50 m x 0.25 m
Columns: Section D = 0.40 m
Modulus of elasticity:
E = 25 GPa, Poisson ratio: ν = 0.3

Constraints: Fixed constraints for the four nodes at the column basis

Loading: Uniform loading
p = 16 kN/m^2 on direction -Z and
p = 16 kN/m^2 parallel to sides AB and DC

Mesh
Shell elements: 15x15 quad elements, the mesh for the triangular elements is obtained from the one for quad elements, by dividing each quad into two triangles.
Beams: Each structural beam is divided into 15 linear beam elements (in accordance with the mesh of the shell elements).

4.4.1 Results for shell elements

The results from the isoparametric shell elements for general use CQUAD4 (4-noded) and CTRIAR (improved triangular) of the program MSC-NASTRAN are used as benchnmarks.

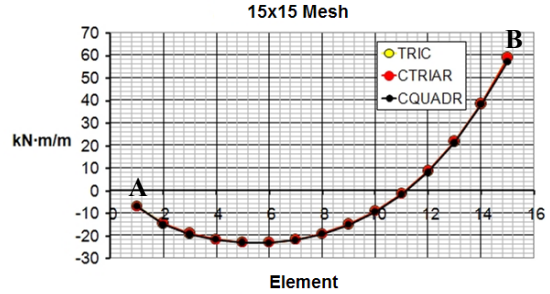

Figure 10. Bending moment $M_{x'x'}$ along the side AB

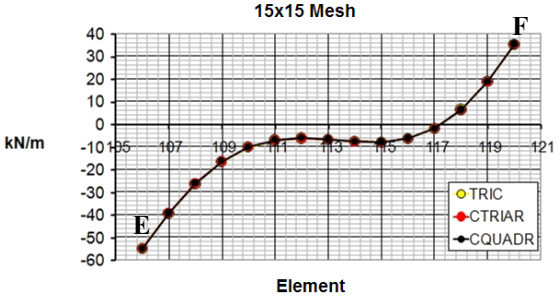

Figure 11. Force $F_{y'y'}$ along the side EF

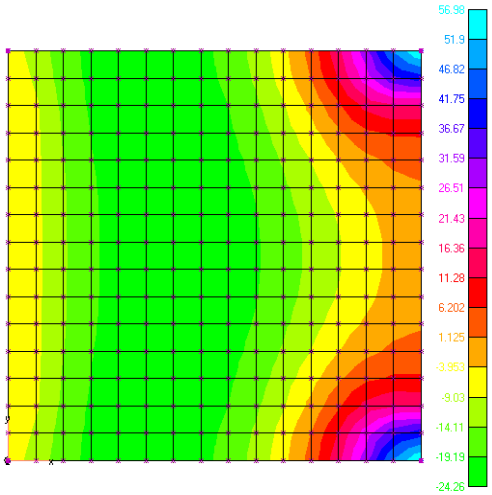

Figure 12. Bending moment $M_{x'x'}$ (N·m/m) (CQUADR elements)

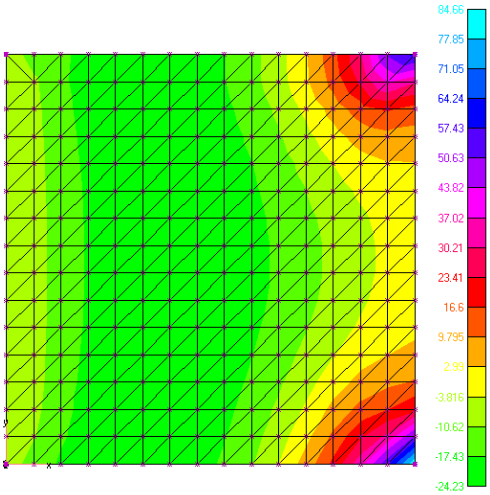

Figure 13. Bending moment $M_{x'x'}$ (N·m/m) (TRIC elements)

4.4.2 Results for beam elements

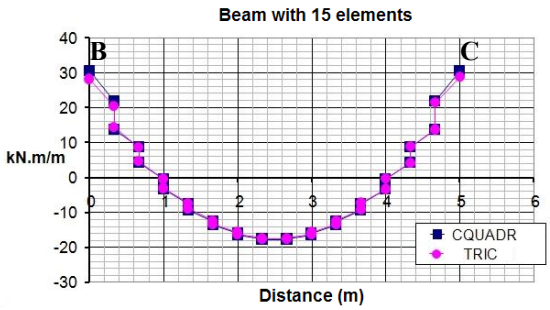

Figure 14. Bending moment M on beam BC

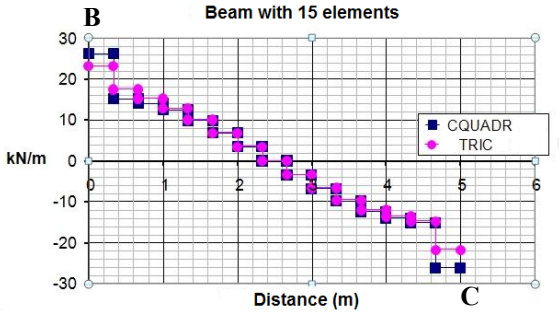

Figure 15. Shear force Q on beam BC

There were small or negligible differences between the results of the analysis with TRIC and MSC-NASTRAN.

4.5 Plate under thermal loading

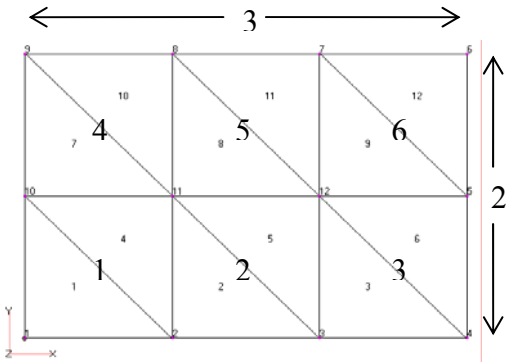

Figure 16. Model for numerical test 5

Finite element mesh
6 quad elements are used. By dividing them into triangles we obtain 12 triangular elements.
Thickness: t = 1.0m

Material
Modulus of elasticity: E = 32 Gpa,
Poisson ratio: ν = 0.25,
Thermal coefficient $\alpha = 10^{-5}$ / °C.

Constraints
All edge nodes are fully constrained.

The results for quad elements using the commercial FE program SOFiSTiK v23 are used as benchmarks.

4.5.1 Uniform thermal loading $\Delta T_N = +20^oC$ for all the structure (membrane mode)

Calculated forces are $F_{xx} = F_{yy} = -8533.33$ kN/m for TRIC, for all elements. The same values are also obtained by SOFiSTiK v23. Other forces (F_{xy}, V_x, V_y) and moments (M_x, M_y, M_{xy}) are equal to zero for all elements, for

both programs. Calculated X and Y constraint forces are $F_x = F_y = 4266.67$ kN/m for TRIC, for all nodes. Corresponding values for SOFiSTiK v23 are $F_x = F_y = 4266.70$ kN/m.

4.5.2 Linear temperature distribution $\Delta T_M = +20^oC$ along the height of the section (bending mode)

Calculated moments are $M_{xx} = M_{yy} = 711.11$ kN·m/m fot TRIC, for all elements. The same values are also obtained by SOFiSTiK v23. Forces (F_x, F_y, F_{xy}, V_x, V_y) and moment M_{xy} are equal to zero for all elements, for both programs. Calculated X and Y constraint moments are $M_x = -M_y = -355.56$ kN·m/m for TRIC, for all nodes. Corresponding values for SOFiSTiK v23 are also $M_x = -M_y = -355.56$.

4.6 Eccentric cantilever beam

The same structure and mesh as in the previous example (Plate under thermal loading) is used. In this case only the side with coordinates y=0.00 is fixed and a compression linear distributed load is applied on the side with coordinates y=2.00 ($P_y = -13.33$ KN/m). Additionally, a z axis eccentricity of the shell's midsurface is set equal to $z_e = -0.50$ m (the reference surface is placed on the structures top fiber). The compression load in combination with the eccentric placement of the reference surface, should lead not only to a compression force of $N_y = -13.33$ kN/m * 3 m = -40.00 kN, but also to a bending moment of magnitude $M_x = -13.33$ kN/m * 3 m * 0.5 m = -20 kNm.

The integration of the element's computed forces is done in two cross sections parallel to the x axis.

Section results	N_y	M_x
y = 0.50 m	-40.00	-20.00
y = 1.50 m	-40.05	-19.96

4.7 Plane frame with shear wall: Shell elements combined with beam elements

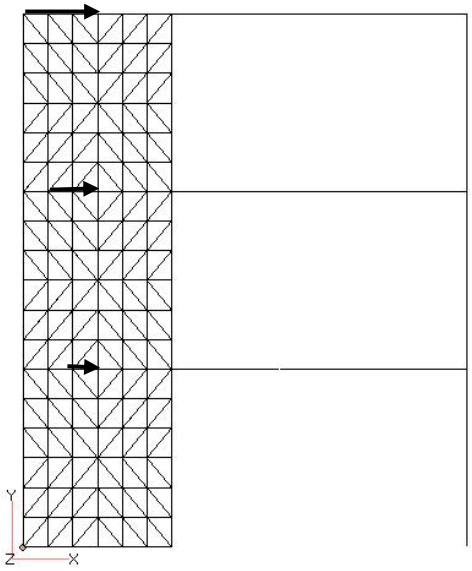

Figure 17. Model for numerical test 7

The plane frame model of Figure 17 consists of a shear wall (height 9 m, width 2.5 m and thickness 0.25 m), three horizontal beams of 5 m length (0.5 m height and 0.25 m width, orthogonal section) and three columns of 3m height each (0.50 m rectangular section). It consists of isotropic material with elastic modulus equal to 30 GPa and Poisson ration equal to 0.20. All base nodes are fully constrained and three concentrated forces of magnitude 20 kN, 40 kN and 60 kN are applied on the center of the shear wall at heights 3 m, 6 m and 9 m, respectively.

Two analyses were carried out, one with the program FESPA and one with MSC-NASTRAN. In both cases the shear wall was modeled with shell elements (TRIC in FESPA and CQUAD4 quadrilaterals in MSC-NASTRAN) and beam elements were used for the beams and the columns. The TRIC element mesh is shown in the figure, while the rectangular mesh was composed of two equal triangles for every quadrilateral element.

In this test example, the TRIC element's ability to fully interact with beam elements is tested. Specifically, the connection between the shell's element azimouthian stiffness term and the beam element's bending term was tested. The reported bending moment of the beam elements from FESPA and MSC-NASTRAN is presented in figures 18 and 19 respectively.

We can see that the TRIC shell elements are capable of transmitting the bending moment to the beams, while the CQUAD4 elements of MSC- NASTRAN fail. The computed top deflection (x-displacement of the top right node) was equal to 0.18 cm for FESPA and 0.19 cm for MSC-NASTRAN.

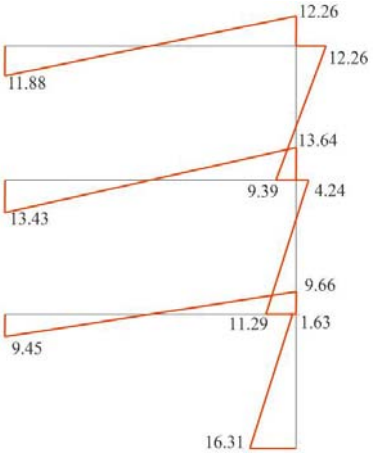

Figure 18. FESPA bending moment diagram.

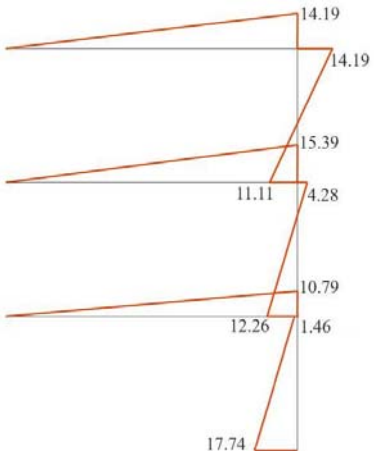

Figure 19. MSC-NASTRAN bending mom. diagram.

5. CONCLUSIONS

From the above test examples a number of concluding remarks can be drawn regarding the TRIC element, its behavior in different kinds of structural problems and its ability to interact with beam elements for structural modeling.

Both stress and displacement fields of the element exhibits similar results compared either to analytical solutions or to those obtained with quadrilateral shell elements of commercial finite element programs. In the test cases where section integration of the element's internal forces field was performed, the results were identical to the ones obtained by the beam theory.

The last example was a test bed for the behavior of the element in case of connecting a beam element in the shell's azimouthian rotational degree of freedom. In this case the beam element's bending moment is computed through the shell's azimouthian stiffness terms. The improved TRIC response was accurate and the bending moment was transmitted to the beam.

ACKNOWLEDGEMENT

The present work is part of a project undertaken by the Institute of Structural Analysis & Seismic Research of the National Technical University of Athens, founded by the company LH Logismiki, in an attempt to integrate the improved TRIC finite element in the commercial structural analysis program FESPA.

The support of the "John Argyris International Centre for Computer Applications in Engineering" is greatly acknowledged. The first author also acknowledges the support of the "John Argyris Foundation".

REFERENCES

[1] A.G. Gisakis, M. Papadrakakis and L. Karapitta (2005), "Improving the performance of the TRIC shell element". *Proceedings of the 5th International Congress on Computational Mechanics (GRACM 05)*, Limassol, Cyprus, 29-30 June 2005, VoII, pp. 821-828.

[2] J.H. Argyris, M. Papadrakakis, C. Apostolopoulou and S. Koutsourelakis (2000), "The TRIC shell element: theoretical and numerical investigation". *Comp. Meth. Appl. Mech. Engrg*, Vol. 182, pp. 217-245.

[3] Argyris, J.H., Tenek, L. and Olofsson, L. (1997), "TRIC: a simple but sophisticated 3-node triangular element based on 6 rigid body and 12 straining modes for fast computational simulations of arbitrary isotropic and laminated composite shells" *Comp. Meth. Appl. Mech. Engrg*, Vol. 145, pp. 11-85.

[4] Argyris, J.H., Tenek, L., Papadrakakis, M. and Apostolopoulou, C. (1998), "Postbuckling performance of the TRIC natural mode triangular element for isotropic and laminated composite shells" *Comp. Meth. Appl. Mech. Engrg*, Vol. 166, pp. 211-231.

[5] Argyris, J.H., Balmer, H., Doltsinis, J.St., Dunne, P.C., Haase, M., Muller, M. and Scharpf, W.D. (1979), "Finite element method – the natural approach" *Comp. Meth. Appl. Mech. Engrg*, Vol. 17/18, pp. 1-106.

[6] Turner, M.J., Clough, R.W., Martin, H.C. and Topp, L.J. (1956), "Stiffness and deflection analysis of complex structures" *J. Aero. Sci*,. Vol. 23, pp. 805–824.

[7] HKS ABAQUS v6.4, Documentation manual (electronic book version).

[8] MSC-NASTRAN 2004, Reference manual (electronic book version).

[9] MacNeal, R.H., Harder, R.L. (1985), "A proposed standard set of problems to test finite element accuracy", *Finite Elements in Analysis and Design*, 1, 3-20.

[10] Charamidopoulos, D., Livieratos S. (2007), "Fespa 7 for Windows Vista", ISBN 960-461-098-8, Kleidarithmos, Athens.